Separation Science and Technology
Publication details, including instructions for authors and subscription information:
http://www.informaworld.com/smpp/title~content=t713708471

Surface Barriers for Retention Enhancement in Field-Flow Fractionation

J. Calvin Giddings[a]; Larell K. Smith[b]; Marcus N. Myers[a]
[a] DEPARTMENT OF CHEMISTRY, UNIVERSITY OF UTAH, SALT LAKE CITY, UTAH [b] Chemistry Department, U.S. Air Force Academy, Colorado

To cite this Article Giddings, J. Calvin , Smith, Larell K. and Myers, Marcus N.(1978) 'Surface Barriers for Retention Enhancement in Field-Flow Fractionation', Separation Science and Technology, 13: 4, 367 — 385

To link to this Article: DOI: 10.1080/01496397808057108

URL: http://dx.doi.org/10.1080/01496397808057108

SEPARATION SCIENCE AND TECHNOLOGY, 13(4), pp. 367–385, 1978

Surface Barriers for Retention Enhancement in Field-Flow Fractionation

J. CALVIN GIDDINGS, LARELL K. SMITH,*
and MARCUS N. MYERS

DEPARTMENT OF CHEMISTRY
UNIVERSITY OF UTAH
SALT LAKE CITY, UTAH 84112

Abstract

It is proposed to modify the surface of a field-flow fractionation (FFF) channel by introducing small barriers perpendicular to flow. Possible advantages include increased retention, sample capacity, and selectivity. It is shown that this approach brings FFF into a closer relationship with chromatography and countercurrent distribution. Approximate theories are developed for retention, plate height, and selectivity, and sources of departure from theory are discussed. Two experimental thermal FFF systems are described, one with barriers established by cutting grooves in a Mylar sheet and another with grooves cut in a copper bar. Despite an observed deviation from the assumed rectangular groove shape, retention enhancement was considerable, and was in reasonable agreement with theory. Plate height, however, greatly exceeded the values observed for nongrooved systems.

INTRODUCTION

As a tool for separating and characterizing heterogeneous mixtures of macromolecules and colloids, field-flow fractionation (FFF) has shown great versatility. Various subclasses of FFF have been applied to species ranging in molecular weight from less than 10^3 to about 10^{12} (*1*). Single runs in thermal FFF have been successful in separating polymers over the

---

*Present address: Chemistry Department, U.S. Air Force Academy, Colorado 80840.

molecular weight range from 4,000 to 7,100,000 in a single programmed operation (*2*).

Despite the inherent versatility of the method, improvements are desirable in a number of performance characteristics. For example, improvements in column efficiency, selectivity, increased sample capacity, and mass range would all add to the potential utility of the method.

In this paper we seek operating improvements through the introduction of migration barriers on the accumulation wall of an FFF channel. These barriers should be small, closely spaced molecule traps that prevent the axial transport of solute near the wall. The downstream displacement of molecules will be momentarily halted when they enter such traps due to the relative stagnancy of fluid within the spaces. Transport would be possible only when diffusion carries individual solute particles above the effective height of the barrier. They may then be carried by axial flow across the barrier, but are subject to repeated detainments behind succeeding barriers.

In this experimental approach, barriers have been created by cutting narrow, parallel grooves in the channel walls perpendicular to the flow direction. The principle is illustrated in Fig. 1. The general concept is, of course, applicable to all types of FFF systems, not just thermal FFF as illustrated in the figure. Barriers might also be created by layers of porous, meshed, or woven material applied to a surface, or a surface might be punctuated by pores or holes.

The above structures are referred to as surface barriers because their function in each case is that of a barrier to axial migration. However, we will use "surface barriers" and "grooves" interchangeably in the general

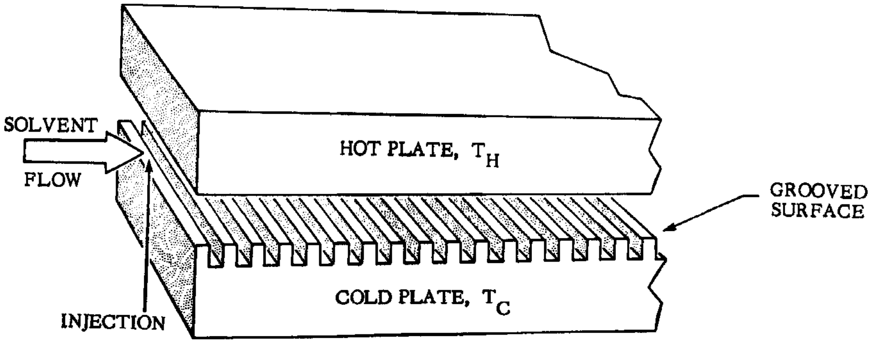

FIG. 1. Schematic of grooved plate thermal FFF column.

discussions of this paper because our specific experimental approach employs grooved surfaces.

The most immediate effect of the grooves, then, will be to increase retention. Due to the fact that in some systems of FFF, such as thermal FFF, fields of adequate strength cannot be generated to retain species of molecular weight below about 10^3, the enhanced retention should aid in extending the effective molecular weight range of the method toward smaller molecules. This approach would complement an earlier approach using increased temperature gradients (*3*).

Another promising aspect of grooved plate columns is the potential for increasing the capacity of the system. Field-flow fractionation is inherently low in capacity, not easily adaptable to large samples. The reason is simply that the entire solute cloud is forced into a very narrow layer against the bottom plate of the column—into a space that is so limited that severe interactions and nonlinearities tend to occur. The grooves of a grooved plate column can be imagined as solute reservoirs which retain solute momentarily while the normal FFF process is proceeding directly overhead. After a short time the solute flowing above the surface will enter one of the grooves through normal mass transport processes, and at the same time some of the solute within the grooves will replace the flowing solute. Thus solute will effectively take turns in undergoing the normal migration process encountered in regular FFF columns. The capacity of the system will be increased roughly by whatever fraction of solute occupies the grooves.

It is clear, of course, that the solute in such a system will move more slowly than that in a normal FFF column and that this will reduce the throughput per unit time of the system. Therefore, the immediate promise of enhanced throughput applies only to the ability to fractionate larger peaks irrespective of time. However, it is important to note that either the throughput per unit time or the fractionation of two peaks hinges on the intrinsic resolving capability of a column. Increased resolution, for example, allows the use of a shorter column and/or a higher flow rate, or both. This is directly beneficial to the throughput per unit time. If, therefore, the surface grooves are capable of enhancing selectivity, and thus resolution, there may be a considerable gain in potential throughput. Below, then, we suggest the third apparent advantage of a barrier system, which is that of the enhancement of selectivity. In the theory section we will note, however, that this may be offset in part by increased peak width.

Solute pulses in FFF are forced by the field against one wall, forming exponential layers. The relative height of the layers for different solutes determines selectivity in normal FFF. With the addition of barriers, selectivity hinges more on the relative fraction of solute left distributed in the space above the barrier height. There is a relatively greater difference in this fraction than in layer height, due to the exponential nature of the distribution. This will be explained in detail in the theory section. The net consequence is that an increased selectivity is expected to accompany the introduction of barriers.

For perspective, it is worth noting that while the barrier system described here is clearly a modified FFF system, it brings FFF into an even closer relationship with chromatography, and it also introduces features resembling those of countercurrent distribution (CCD) systems. The chromatography analogy results from the fact that one is creating pools of stationary liquid within the grooves, and that migration is affected by different levels of partitioning between these stationary pools and the adjacent moving liquid. The amount partitioned in the stationary liquid depends on its amount (groove size) as in chromatography, but is fundamentally controlled by field strength rather than by chemical forces. An interesting system would, of course, result if the grooves were filled with a second phase so that partitioning would be controlled by a combination of chemical forces and external fields.

The surface barrier FFF system resembles CCD by its introduction of regular fixed partitioning chambers undergoing repeated equilibrations with a phase passing overhead. The chambers in the FFF system are, of course, much smaller and more numerous, promoting rapid equilibration and resolution. Again the partitioning is controlled by field intensity rather than by chemical forces.

In the theory section which follows, we will describe two limiting cases for grooved surfaces. These correspond, essentially, to grooves cut in good heat conductors and poor heat conductors, respectively. An attempt to approach the behavior of both cases will be described in the experimental section.

THEORY

Figure 2 defines the important dimensions of the model system. Two limiting cases can be distinguished that depend on groove dimension and column materials. In Case I, the field or gradient drives the particles or molecules toward $x = 0$ but no further. Mass transport within the grooves ($x < 0$) is driven by diffusion only. This case would be approached, for

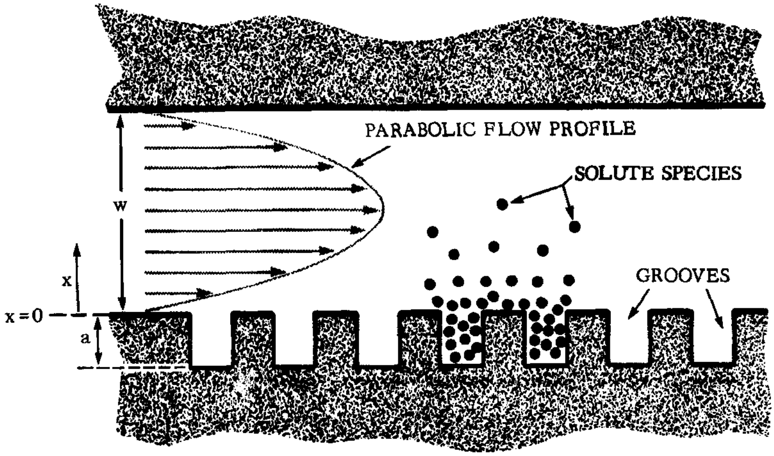

Fig. 2. Side view of grooved FFF column.

example, for deep, narrow grooves in a metallic plate used for thermal FFF, because in such grooves the temperature gradient would be negligible.

Case II is based on an external gradient maintained all the way across the channel ($w > x > 0$) and the groove space ($0 > x > -a$). This would be realized for grooves cut in a material with a thermal conductivity equal to that of the liquid carrier, or approximately for grooves whose width greatly exceeds their depth.

For both Cases I and II, we employ simplifying assumptions in order to derive a first approximation to retention. First, we assume that the flow in the channel ($w > x > 0$) is unchanged by the presence of the grooves. Such flow will normally approximate a parabolic form, as shown in Fig. 2. Second, we assume that there is zero flow within the grooves. Third, we assume that steady-state concentration levels are established along coordinate x.

The flow assumptions are clearly in error, but difficult to treat exactly. The channel flow will sag into the grooves making them, in effect, more shallow. Rotational currents will also be established in the grooves, and, if significant, they will aid mass transport and, in Case II, reduce retention.

The above perturbations to our model will be reduced by employing small, deep pores. With reasonable care in limiting ourselves to compatible experimental systems, the simple approach developed here should form an adequate base on which to judge the potential value of the approach.

Retention in Case I

The steady-state distribution of solute in the channel will be exponential, the same as that in nongrooved FFF channels (*4*).

$$c = c_0 \exp(-x/l) \qquad (w > x > 0) \tag{1}$$

In this equation, c_0 is the concentration, c, at $x = 0$, and l is termed the mean thickness of the solute layer in the channel.

Within the grooves the concentration will assume a constant value in equilibrium with the channel concentration at $x = 0$:

$$c = c_0 \qquad (0 > x > -a) \tag{2}$$

Specification of the concentration distribution, above, makes it possible to determine the fraction F_w of solute remaining in the channel. We have the general expression

$$F_w = \frac{\int_0^w c\,dx}{\int_0^w c\,dx + f\int_{-a}^0 c\,dx} \tag{3}$$

where f is the grooved fraction, or, for other porous surfaces, the fraction of space accessible to the solute between $x = -a$ and $x = 0$. Substitution of Eqs. (1) and (2) into the integrals of Eq. (3), followed by integration, yields

$$F_w = \frac{1 - \exp(-1/\lambda)}{1 - \exp(-1/\lambda) + fa/l} \tag{4}$$

where λ is the dimensionless ratio l/w.

Solutes that are inert and thus not retained (not influenced by the field) are characterized by $\lambda = \infty$. In this limit, F_w becomes

$$F_w = \frac{w}{w + fa} \tag{5}$$

The retention ratio in the grooved plate system, R_g, can be defined as V/V_{inert}, where the two V's define the mean velocity of the actively retained and inert solute peaks, respectively. Each V can be written as the product

$$V = V_w F_w \tag{6}$$

For the inert peak, V_w is simply the mean velocity $\langle v \rangle$ of carrier in the channel. Thus, with the aid of Eq. (5), we get

$$V_{\text{inert}} = \langle v \rangle w/(w + fa) \tag{7}$$

For the retained peak, V_w is $R_0\langle v \rangle$, where R_0 is the retention ratio applying to a nongrooved column of the same dimensions and gradients. [Quantity R_0 is given by standard equations (*4*).] Combining this part with Eq. (4), and substituting both in Eq. (6), we find

$$V = \frac{R_0\langle v \rangle[1 - \exp(-1/\lambda)]}{1 - \exp(-1/\lambda) + fa/l} \tag{8}$$

In that $R_g = V/V_{\text{inert}}$, we obtain

$$R_g = \frac{R_0(w + fa)[1 - \exp(-1/\lambda)]}{w(1 - \exp(-1/\lambda) + fa/\lambda w)} \tag{9}$$

where λw has been substituted for l.

The ratio R_g/R_0 indicates the degree to which peak velocity has been decreased (retention increased) by the grooves. From Eq. (9), this ratio is

$$\frac{R_g}{R_0} = \frac{(w + fa)[1 - \exp(-1/\lambda)]}{w(1 - \exp(-1/\lambda) + fa/\lambda w)} \tag{10}$$

Retention in Case II

The treatment of Case II proceeds much like that for Case I. Equation (1) applies over both channel and grooves, and is thus valid from $x = -a$ to $x = w$. Equation (2) is, of course, not applicable. The integrations required by Eq. (3), therefore, lead to a result for F_w slightly different from that shown in Eq. (4):

$$F_w = \frac{1 - \exp(-1/\lambda)}{1 - \exp(-1/\lambda) + f[\exp(a/\lambda w) - 1]} \tag{11}$$

Equations (5), (6), and (7) maintain their validity, but the last term in the denominator is modified as shown for Eq. (11). This change carries over to Eqs. (9) and (10). Hence the ratio R_g/R_0 for Case II is of the form

$$\frac{R_g}{R_0} = \frac{(w + fa)[1 - \exp(-1/\lambda)]}{w(1 - \exp(-1/\lambda) + f[\exp(a/\lambda w) - 1])} \tag{12}$$

Peak Width

No rigorous treatment of peak spreading will be attempted here. However, the importance of peak width to the ultimate goals of the present system is such that a brief discussion is merited.

The asymptotic theory of peak dispersion in nongrooved systems leads to a plate height which under conditions of high field strength approaches (*5*)

$$H = 24\lambda^3 w^2 \langle v \rangle / D \tag{13}$$

where D is the diffusion coefficient for the solute. This plate height accounts for diffusive equilibration across the thickness of the solute layer as it is compressed by the field.

It is useful to invoke the analogy between FFF and chromatography for the surface barrier system proposed here. The channel liquid may be thought of as the mobile phase and the groove liquid as the stationary phase, as noted. In chromatographic systems there is a plate height contribution from both phases, and the same is expected here. Equation (13) will represent the "mobile phase" contribution under conditions of zero "stationary phase" influence. In chromatographic systems an increase in retention by the stationary phase ordinarily increases the mobile phase contribution as well (*6*). For a capillary tube the increase is 11-fold in going from no retention to complete retention. A similar occurrence is expected with FFF. Therefore, the "mobile phase" or channel contribution in FFF is expected to assume the form

$$H = 24\theta(F_w)\lambda^3 w^2 \langle v \rangle / D \tag{14}$$

where $\theta(F_w)$ is a function that will increase as the fraction F_w of solute in the channel falls below unity. For the capillary tube this function is $\theta(F_w) = 6F_w^2 - 16F_w + 11$, an approximation that may suffice for FFF until a more rigorous treatment is undertaken.

The groove or "stationary phase" contribution should agree rather precisely with the analogous chromatographic system for Case I. For grooves uniform along their entire depth, we would have (*6*)

$$H = \frac{2}{3} F_w(1 - F_w) a^2 \langle v \rangle / D \tag{15}$$

This equation may crudely approximate most Case II systems as well.

The H term of Eq. (15) will increase rapidly as the groove depth, a, increases. Thus groove depth must be limited or sacrifices in resolution will occur. Whether this limitation will significantly interfere with the major goals of a grooved plate system is a question that must await a more detailed analysis. It is clear, however, that the increase in one plate height term and the addition of another raises important barriers to the practical operation of such systems.

Resolution

It has been shown that the resolution of two peaks in thermal FFF can be expressed as (*7*)

$$R_s = \left(\frac{N}{16}\right)^{1/2}\left(\frac{d\ln R}{d\ln\lambda}\right)\left(\frac{\Delta\alpha}{\alpha}\right) \tag{16}$$

with the three terms on the right representing, respectively, column efficiency as reflected by the number of plates N, the fractional gain in R relative to the fractional increase in λ, and the selectivity between components as measured by the fractional increment $\Delta\alpha/\alpha$ in the thermal diffusion factor α. For two specified components run on two different columns having the same number of theoretical plates, the difference in resolution in the columns will be dependent only on the $d\ln R/d\ln\lambda$ term. This term can be obtained rather easily in the case of high field strength and strong retention ($\lambda \rightarrow 0$). In this limit we may use the approximations $R_0 = 6\lambda$ (*4*) and $\exp(-1/\lambda) = 0$. These approximations used in conjunction with Eq. (9) lead to

$$\ln R_g = \ln(6/w)(w + fa) + \ln\lambda - \ln(1 + fa/\lambda w) \qquad \text{(Case I)} \tag{17}$$

We noted in the *peak width* subsection that groove depth a may be required to be small. Thus fa may be larger, smaller, or comparable to $\lambda w = l$. However, in order to see much effect due to the grooving, fa must be $\sim\lambda w$ or $>\lambda w$. In the extreme case in which nearly all solute is in the grooves, $fa \gg \lambda w$, Eq. (17) becomes

$$\ln R_g = \ln(6/w)(w + fa) + \ln\lambda - \ln(fa/\lambda w) \qquad \text{(Case I)} \tag{18}$$

We obtain

$$\frac{d\ln R_g}{d\ln\lambda} = 2 \qquad \text{(Case I)} \tag{19}$$

For barrier-free FFF, for which we can use $R = 6\lambda$ under high field conditions, $(d\ln R/d\ln\lambda) = 1$. Thus the grooves create a twofold increase in intrinsic resolution under the prescribed conditions for Case I. However, as we have noted, there may be fewer theoretical plates in a channel with barriers, so the advantages may be offset. Equation (16) shows that the nongrooved column would require four times more plates to offset the twofold increase in $d \ln R/d \ln \lambda$ accompanying the grooved system.

Case II can be treated similarly. Using essentially the same assumptions, we get

$$\ln R_g = \ln (6/w)(w + fa) + \ln \lambda - \ln (f - a/\lambda w) \qquad \text{(Case II)} \qquad (20)$$

This equation yields

$$\frac{d \ln R_g}{d \ln \lambda} = 1 + a/w\lambda \qquad \text{(Case II)} \qquad (21)$$

Under the assumed conditions, $fa \gg w\lambda$, which is equivalent to $a \gg w\lambda$ because $f < 1$, Eq. (21) shows a very substantial enhancement in intrinsic resolution over the nongrooved systems. This result is sufficiently encouraging to make the further investigation of surface barrier FFF worthwhile, despite the questions we have raised about increases in peak width.

Basis of Increased Selectivity

The enhanced resolution predicted by Eq. (21) has a simple origin in the relative behavior of two exponential curves representing the concentration profiles of two solutes. Each exponential has the form of Eq. (1), except that the two solutes are characterized by two different l values, l_1 and l_2. The fraction of such an exponential distribution lying above a barrier of height a, and thus the fraction in a position to move forward in the channel, can be shown to equal

$$\text{fr}\,(x > a) = \exp\,(-a/l) \qquad (22)$$

The ratio of such fractions for two different l values is

$$\frac{\text{fr}_2\,(x > a)}{\text{fr}_1\,(x > a)} = \exp\left(\frac{a}{l_1} - \frac{a}{l_2}\right) \qquad (23)$$

If we write $l_2 = l_1 + \delta l$, where δl is small because the two solutes are assumed to be similar in properties, we arrive at the approximation

$$\frac{\text{fr}_2\,(x > a)}{\text{fr}_1\,(x > a)} = \exp\,(a\delta l/l_1^2) \qquad (24)$$

In other words, given fixed solutes and thus fixed values of l_1, l_2, and δl, the relative fraction above height a increases exponentially with the magnitude of *a*. Thus relative migration and its associated resolution are enhanced with increasing barrier height. While this result reflects the properties of exponential distributions, which are always most selective at their extremes, optimism must, as before, be tempered by the knowledge that increasing peak width and decreasing migration rate will also accompany increases in barrier height *a*.

EXPERIMENTAL

Except for the grooving, the columns and ancillary apparatus used in this study were the same as those previously described (*8*). Two columns were used. A *Mylar* column (corresponding roughly to theoretical Case II) consisted of a standard copper apparatus with a strip of 0.127 mm thick Mylar glued to the bottom (cold) plate. The Mylar had grooves cut in it with a milling machine especially adapted to the purpose. The grooves were of nominal dimensions 0.05 mm in depth and width, and spaced 0.05 mm apart. They were cut perpendicular to the direction of carrier flow. A Mylar spacer, from which the channel had been cut, was placed on top of the grooved Mylar surface to create a channel with the nominal dimensions 0.0254 × 37 × 1.75 cm^3. Because the adhesive (3M Vinyl Adhesive 1099) used to cement the Mylar to the bottom plate is somewhat plastic, even after a heating-compression treatment before grooving, the actual column width was probably about 10% less than the nominal dimension of the Mylar: 0.23 mm instead of 0.254 cm. No compression of the Mylar itself has ever been observed with the pressures normally imposed on the spacer (1800 to 3000 psi).

The Mylar spacer material has a similar thermal conductivity to that of the solvent employed (ethyl benzene): 3.4×10^{-4} vs 3.16×10^{-4} cal/cm-sec°C, respectively. This made conditions suitable for Case II theory. The measurement of temperature was made at the surface of the copper plate, however, so that calculations of the temperature drop ΔT across the channel had to take account of the temperature drop across the Mylar.

The *copper* column (corresponding to theoretical Case I) was identical to the Mylar column in general configuration, but the grooves were cut in the copper bar itself. The nominal groove dimensions were identical to those for column number 2. The channel dimensions were 0.0254 × 40.2 × 2.0 cm^3.

The solutes were linear polystyrene polymers obtained from Pressure Chemical Company. The reported M_w/M_n ratios were in the range 1.06 to 1.13. Injections were made with Hamilton microliter syringes. Solute concentrations in the injected solution were in the range 0.01 to 0.03 mg/μl. The samples injected were 1 to 6 μl in volume.

In order to establish reasonable parameters for comparison with the theoretical models, actual groove dimensions were required. These dimensions for both the Mylar and metal systems were established by casting latex silicone rubber flexible molding compound (General Electric RTV 700) on the surfaces, and stripping after curing. The mold thus obtained was sliced perpendicular to the grooves, and photomicrographs were obtained of the slices. A scale was established by photographing a standard grid with the same microscope settings. The dimensions of the grooves were then obtained by measuring the photographs with a precision ruler.

RESULTS AND DISCUSSION

Figure 3 is a photomicrograph of the two groove structures. It shows that the groove configuration deviates significantly from the model structure of rectangular grooves. Furthermore, the grooves in the Mylar were deeper than expected, while those in the copper were shallower.

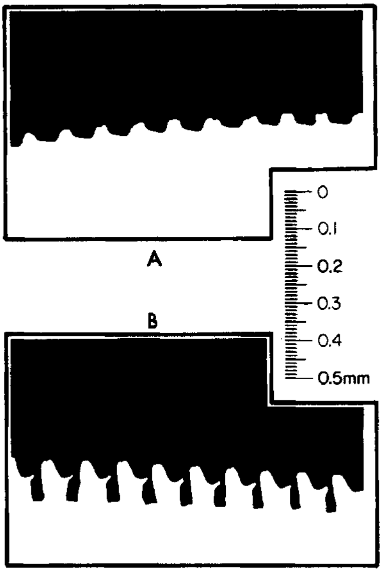

FIG. 3. Photomicrograph of grooved surfaces. The dark part is the casting and the light part thus represents the solid material in which grooves are cut. (A) copper, (B) Mylar. A scale is shown.

These departures complicate the quantitative study of retention. Nonetheless, they constitute legitimate surface barriers which can be used to establish the main trends of performance in surface barrier FFF systems.

Figure 4 illustrates the capability of the Mylar system to operate as a retention device. Substantial retention is shown to exist for 20,400 molecular weight polystyrene, even though the temperature drop ΔT between walls was only 35°C.

Table 1 summarizes the data acquired from such retention measurements using polymers of different molecular weights and different ΔT's. The ΔT values reported are those applied across channel width w. A correction was applied to the Mylar system to account for the finite temperature drop across the Mylar layer.

In order to show how dimensional changes in the grooves are expected to shift retention behavior, in Fig. 5 we have plotted retention ratio R_g against λ for various examples of Case II grooves. The retention ratio R_0 of a nongrooved channel is shown for comparison. The increase in retention (decrease in R) due to grooving is striking. The deepest grooves, of course, show the strongest effect.

In order to bring about some correspondence between the odd-shaped grooves of our experimental systems and the model rectangular grooves, we have used several equivalent groove dimensions. Except as noted, we have let groove depth a equal the depth averaged over the bottom of the groove. Fraction f, by our definition, has been taken as the fractional area belonging to the groove over its full depth a. Using Fig. 3, we obtain a = 0.032 mm and $f = 0.57$ for the copper grooves and a = 0.106 mm and $f = 0.38$ for the Mylar grooves.

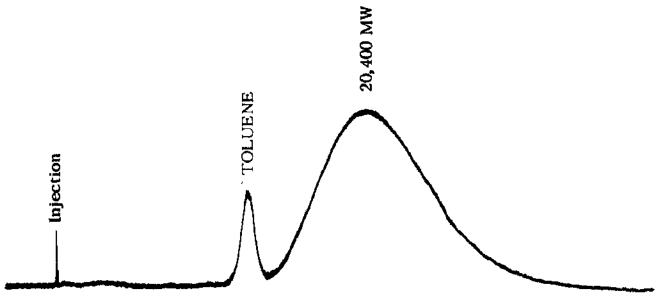

FIG. 4. Retention of 20,400 MW polystyrene in the Mylar grooved system with T = 35°C, T(hot) = 52°C, and V_{inert} = 0.018 cm/sec. Toluene can be considered as an "inert" peak.

TABLE 1

Retention Data for Copper Column and Mylar Column as a Function of the Temperature Increment ΔT across the Channel. The Associated λ Value is Shown. The Molecular Weight of the Linear Polystyrenes is Shown in the First Column

MW	ΔT (°C)	λ	R_g
Copper column			
3,525	60	.41	.85
	80	.31	.77
	40	.62	.91
	50	.49	.88
	65	.38	.81
10,300	30	.47	.88
	40	.35	.82
	50	.28	.79
	60	.23	.70
	65	.22	.68
	80	.17	.60
20,400	30	.31	.79
	40	.24	.70
	60	.16	.57
	65	.14	.51
	70	.13	.47
	80	.11	.43
51,000	30	.18	.62
	40	.14	.51
	50	.11	.45
	60	.09	.38
	65	.08	.32
Mylar column			
2,100	54	.69	.83
4,000	54	.46	.75
10,300	50	.28	.62
	42	.34	.65
	50	.19	.49
	24	.39	.73
	35	.27	.62
37,000	15	.44	.77
	24	.27	.63
51,000	20	.27	.61

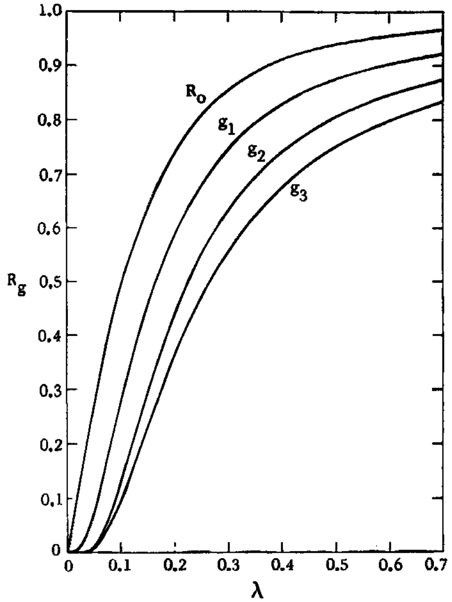

FIG. 5. Theoretical retention ratios for a nongrooved system (R_0) and three Case II grooved systems (g_1, g_2, g_3). Groove parameters are $a = 0.0254$ mm and $f = 0.5$ for g_1, $a = 0.0508$ mm and $f = 0.5$ for g_2, and $a = 0.0508$ mm and $f = 0.8$ for g_3.

Departures from theory are, of course, expected when the grooves are not deep rectangles. Some hydrodynamic perturbations for shallow grooves were mentioned in the theory section. These are expected to reduce retention. In addition, shallow grooves in a conducting (Case I) surface will tend to establish temperature gradients in their interior parts not adjacent to the walls, and the normal temperature gradient in the channel will be perturbed above the groove for a distance equal to several groove widths. Thus these grooves would be expected to behave in an intermediate way between Case I and Case II.

Departure from a rectangular groove shape in Case I will have little effect on retention, but it will affect peak width. Triangular grooves will have a decreased plate height relative to rectangular grooves having the same parameters. Grooves with bottlenecks or obstructions will have an increased plate height. The principles defining these departures will be essentially equivalent to those existing for nonuniform pores in the stationary phase of chromatographic systems (*6*).

Case II systems will exhibit plate height departures similar to Case I systems for nonrectangular grooves. In addition, retention will be changed. Grooves converging toward the bottom will have decreased retention while diverging grooves will have a greater retention than the standard rectangular pore. This is a consequence of the exponential distribution extending into the groove, giving added weight, insofar as retention is concerned, to the deepest part of the groove.

With the above limitations in mind, we show in Fig. 6 our experimental data for the two systems plotted against λ. Several corresponding theoretical curves are also shown. For the copper system, we have calculated retention according both to Case I (Eq. 10) and Case II (Eq. 12), inasmuch as the experimental circumstances are intermediate between the two as noted earlier. These are shown as Curves Ia and IIa in the plot. Both overestimate retention. This is most likely a consequence of the hydrodynamic effect in which flow streamlines sag into shallow grooves and sweep out much of

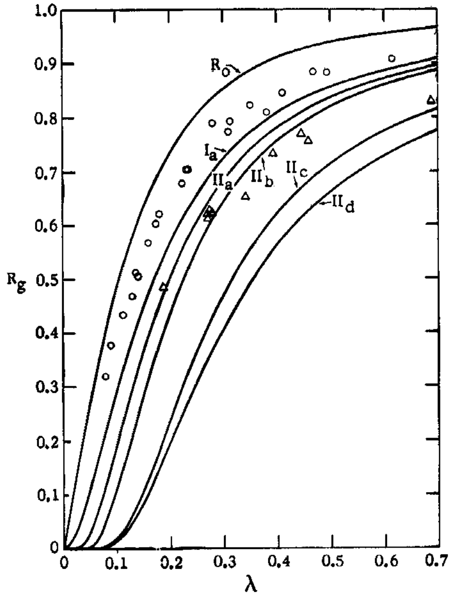

FIG. 6. Experimental retention ratio R_g for the copper system (circles) and the Mylar system (triangles). The theoretical curves, from top to bottom, are for the nongrooved system (R_0); Case I, $a = 0.032$ mm, $f = 0.57$ (Ia); Case II, $a = 0.032$ mm, $f = 0.57$ (IIa); Case II, $a = 0.063$ mm, $f = 0.27$ (IIb); Case II, $a = 0.106$ mm, $f = 0.27$ (IIc); and Case II, $a = 0.106$ mm, $f = 0.38$ (IId).

their solute. This would tend to reduce the volume of liquid that could be considered stagnant, and would thus reduce retention, in accord with the results.

The Mylar system is clearly more difficult to simulate because of the odd groove shape. We have tried several sets of groove parameters derived from the photomicrograph of Fig. 3. The retention curves of Fig. 6 corresponding to these parameters, all from Case II theory, are shown as IIb, IIc, and IId. The last corresponds to the average depth and fractional width measurements noted previously. This curve clearly overestimates retention. A probable explanation lies in the above discussion of nonrectangular groove effects.

Observation of Fig. 3 shows that the grooves are much narrower at the bottom than at the top. In effect, they converge in an irregular way toward the bottom. The effective removal of "deep" groove space will reduce retention, as noted in the discussion and as observed in Fig. 6.

Compensation for the above effect can be made by assuming a fractional groove area or width corresponding only to the deep slot below the "thumb" $f = 0.27$, instead of the average value $f = 0.38$. This change leads to Curve IIc, a plot which agrees better with observations but which still overestimates retention.

It is also likely that the wide upper part of each Mylar groove acts as a shallow pore, largely swept out by solvent. This would reduce the effective depth of the groove. If we assume that the depth is that from the "thumb" to the bottom, $a = 0.063$ mm, in place of the overall depth, $a = 0.106$ mm, we obtain Curve IIb. This is in fair agreement with experiment, particularly at the smaller λ values.

While our choices of parameters are somewhat arbitrary, the above manipulations show that the experimental results can be described using parameters of a reasonable magnitude. The overall agreement of theory and experiment, considering the approximations, is reasonable.

It would, of course, be desirable to extend this test to other groove dimensions and to cases of higher retention than those represented by $R \sim 0.3$. It would be especially useful to employ grooves with a true rectangular shape.

The width of the peak illustrated in Fig. 4 is excessive by normal FFF standards. This can be explained in part by reference to the appropriate part of the theoretical discussion. However, the small, unexplained "thumb" shown protruding into the Mylar groove in Fig. 3 undoubtedly restricts transport in and out of the groove and further increases the plate height beyond that for nongrooved FFF columns.

Figure 7 compares plate height H versus flow velocity $\langle v \rangle$ curves for the Mylar system and a nongrooved channel having the same dimensions. It is clear that peak broadening in the grooved system is excessive at all measured velocities.

In conclusion, we find that retention is increased more or less as expected in our experimental systems. This confirms in an indirect way the postu-

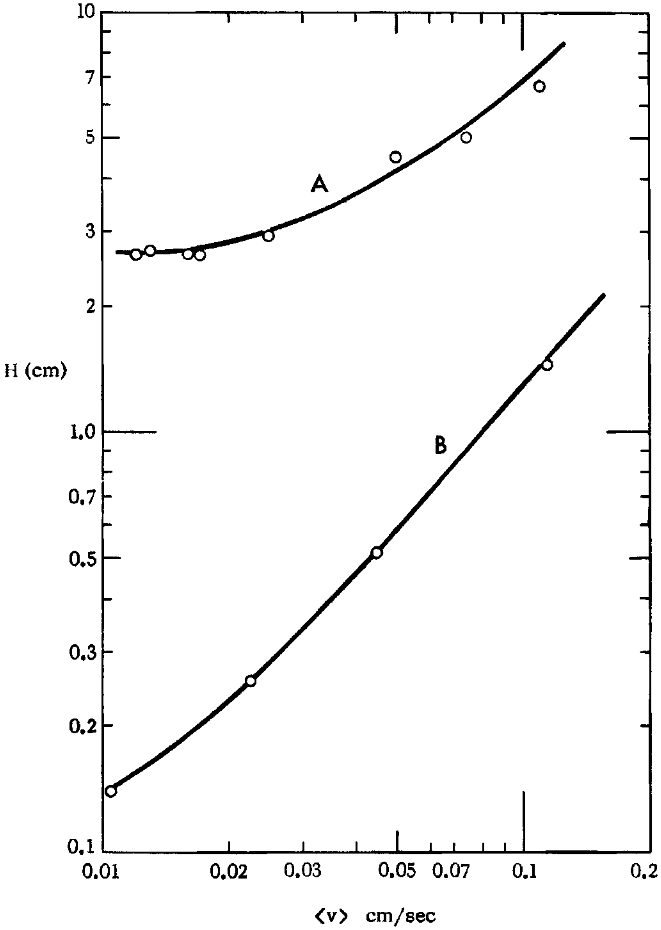

FIG. 7. Comparison of plate height curves for 20,400 MW polystyrene in (A) Mylar grooved system and (B) nongrooved system. $\Delta T = 50°C$, $R_g = 0.51$ (A) and 0.76 (B).

lated increase in selectivity, in that the selectivity argument was based on the expected retention behavior. However, a great deal more work is needed in designing systems with increased peak sharpness and resolution in order to reach the practical goals outlined at the beginning of this paper.

Acknowledgment

This investigation was supported by Public Health Service Research Grant GM 10851-20 from the National Institutes of Health.

REFERENCES

1. J. C. Giddings, *J. Chromatogr.*, *125*, 3 (1976).
2. J. C. Giddings, L. K. Smith, and M. N. Myers, *Anal. Chem.*, *48*, 1587 (1976).
3. J. C. Giddings, L. K. Smith, and M. N. Myers, *Ibid.*, *47*, 2389 (1975).
4. J. C. Giddings, *J. Chem. Educ.*, *50*, 667 (1973).
5. J. C. Giddings, Y. H. Yoon, K. D. Caldwell, M. N. Myers, and M. E. Hovingh, *Sep. Sci.*, *10*, 447 (1975).
6. J. C. Giddings, *Dynamics of Chromatography*, Dekker, New York, 1965, Chap. 4.
7. J. C. Giddings, Y. H. Yoon, and M. N. Myers, *Anal. Chem.*, *47*, 126 (1975).
8. J. C. Giddings, F. J. F. Yang, and M. N. Myers, *Sep. Sci.*, *10*, 133 (1975).

Received by editor June 6, 1977